Available online at www.sciencedirect.com
SCIENCE DIRECT®
Acta Materialia 52 (2004) 3737–3744
Acta MATERIALIA
www.actamat-journals.com

Creep behaviour of Ni-base single-crystal superalloys with various γ' volume fraction

Takao Murakumo *, Toshiharu Kobayashi, Yutaka Koizumi, Hiroshi Harada

High Temperature Materials 21 Project, National Institute for Materials Science (NIMS), 1-2-1 Sengen, Tsukuba Science City, Ibaraki 305-0047, Japan

Received 2 April 2003; received in revised form 16 April 2004; accepted 27 April 2004

Abstract

Creep tests at 900 °C, 392 MPa and 1100 °C, 137 MPa were performed on a third generation Ni-base single-crystal superalloy TMS-75 and its γ/γ' tie line alloys. These tie line alloys were designed to contain various volume fractions of γ', while the compositions of two individual phases were kept the same. The longest rupture life was attained by an alloy with γ' content in vicinity of 65% in both creep condition, which is similar trend has been observed in polycrystalline Inconel 713C through an earlier study by one of the authors. However, in comparison with measured amount of γ', the creep rupture lives were the longest at about 70% and 55% measured γ' volume fraction at 900 and 1100 °C, respectively. In addition, the dependence of the creep rupture life on the amount of γ' was more evident in single crystal than in polycrystal. Rafting was observed in the ruptured 80% γ' alloy in the direction parallel to the stress axis, unlike the rafting commonly observed in the 40–60% γ' alloys, perpendicular to the loading axis. This parallel raft structure can be explained by the interchanges in the relative roles of the matrix and the dispersed phase.

Keywords: Nickel alloys; Creep; Scanning electron microscopy; Rafting; Superalloy

1. Introduction

Ni-base superalloys for gas turbine blades have developed over the years, as a mean of raising the thermal efficiency in aero engines and in gas turbines for power generation. Common superalloys consist of γ and γ' phases, with a face-centered cubic and $L1_2$ structures, respectively. It was first reported by one of the authors (Harada [1,2]) that the creep rupture life was the longest in the vicinity of 65% γ' under any creep condition in polycrystalline Ni-base superalloy Inconel 713C. This tendency was expected to be applicable to single-crystal superalloys and in fact, many studies at around 60–70% in γ' fraction have been carried out in last two decades to find the optimum chemical composition of Ni-base superalloys. However, when the composition of each phase varies, it is difficult to evaluate only the effect of the changes in the γ' fraction because the strength of each phase and the lattice misfit should also change. Therefore, as tie line single-crystal superalloys contains different γ' volume fractions with the same compositions of each phase, an investigation using these alloys is expected to produce results of great importance.

Fig. 1 shows a pseudo-binary phase diagram for a (Ni, X)–(Al, Y) system. Now, assuming that a Ni-base superalloy has a composition indicated by A in Fig. 1 and consists of a γ/γ' two-phase structure in equilibrium at a given temperature, then the compositions of the γ and γ' phase in this alloy should be indicated by B and C. In other words, any alloys on the tie line BC can be made from mixing two alloys having the composition B and C. This logic can be applied to multi-component systems. When the compositions of γ and γ' are given as X_i and X_i' respectively, the composition (C_i) of a Ni-base superalloy for a given γ' fraction (f)

* Corresponding author. Tel.: +81-298-592-516; fax: +81-298-592-501.
E-mail address: murakumo.takao@nims.go.jp (T. Murakumo).

1359-6454/$30.00 © 2004 Acta Materialia Inc. Published by Elsevier Ltd. All rights reserved.
doi:10.1016/j.actamat.2004.04.028

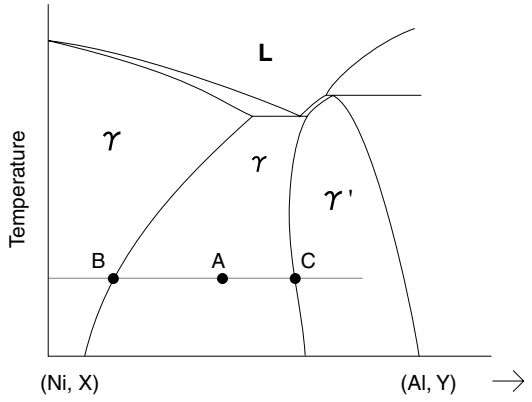

Fig. 1. Schematic drawing of pseudo-binary phase diagram for (Ni, X)–(Al, Y) system.

is obtained by Eq. (1), which is the equation of a tie line representing the compositions of γ and γ' in a state of equilibrium,

$$C_i = (1-f)X_i + fX_i' \quad (i:\ Ni,\ Al,\ Co,\ Cr,\ Mo,\ etc.). \tag{1}$$

In this study, the creep behaviour and microstructure evolution during creep in Ni-base single-crystal superalloys with various γ' fractions are investigated.

2. Material and experimental procedure

The equilibrium compositions of the γ and γ' phases in the third generation single-crystal superalloy TMS-75 [3] were calculated using the alloy design program (ADP) [4,5] which was developed at NIMS in Japan, as shown in Table 1. First, the γ and γ' single-phase alloys were cast as master alloys. These alloys were mixed to make six single-crystal superalloys which had been designed to contain 0, 20, 40, 60, 70, 80 and 100 at.% γ' phase at 900 °C. For consistency, each alloy is henceforth referred to in terms of the originally designed γ' volume fraction values, e.g., 20% γ', etc. The original TMS-75 containing 65% γ' is referred to as "standard TMS-75" in this study. The single crystals were produced in a directional solidification furnace in the form of bars with a diameter of 10 mm. The longitudinal direction was near [0 0 1] for the 0–80% γ' alloys, whereas for 100% γ', it was near [1 1 1], according to the preferred growth direction of the primary crystal. Solution treatment and two-step aging heat treatment were carried out on each alloy under an optimum condition for standard TMS-75 as follows:

1300°C, 1 h + 1320°C, 5 h
→ GFC (Gas Fan Cool) → 1120°C, 5 h → GFC
→ 870°C, 20 h → GFC

Constant load tensile creep tests were then performed at 900 °C, 392 MPa and 1100 °C, 137 MPa. After the heat treatment and creep rupture, SEM studies were carried out.

3. Experimental results

3.1. Microstructure after heat treatment

Fig. 2 shows the as-heat-treated microstructure of each alloy. The 0% γ' fraction alloy consists mostly of a single γ phase; however, a very small amount of γ' was observed, particularly in the interdendritic areas. In the 20% γ' alloy, fine spherical γ' precipitates were observed (Fig. 2(b)). The spherical shape smaller γ' precipitates is derived from the relatively large interfacial energy in comparison to the elastic strain energy. The size of these randomly distributed precipitates is approximately 25–50 nm. This microstructure suggests that the 20% γ' alloy consisted of only a γ phase during the first aging heat treatment at 1120 °C. In the case of the 0% and 20% γ' fraction, the actual volume fraction of γ' in the interdendritic regions was somewhat larger than that in the dendrites due to the segregation, during solidification, of refractory elements. Fig. 2(c) shows the as-heat-treated microstructure of the 40% γ' alloy. Cuboidal γ' precipitates with sides of 200–500 nm were aligned along $\langle 1\,0\,0 \rangle$ during the aging treatment because of the elastic interaction between precipitates. Many fine spherical γ' particles, which have precipitated in the second step aging treatment at 870 °C for 20 h, were also observed among the cuboidal γ' precipitates. In the 60% γ' alloy, as shown in Fig. 2(d), the microstructure was coherent γ/γ' two-phase structure as in standard TMS-75, and other modern Ni-base superalloys. There were no significant differences between the dendritic and interdendritic regions in the 40% and 60% γ' alloys. The γ' volume fraction of the as-heat-treated microstructures was in accordance with the calculated value for the 0–60% γ' alloys.

Table 1
Chemical composition (wt%) of γ and γ' phases in TMS-75 calculated by ADP

	Ni	Co	Cr	Mo	W	Al	Ta	Hf	Re
Standard TMS-75	59.90	12.00	3.00	2.00	6.00	6.00	6.00	0.10	5.00
γ phase	52.05	17.85	5.87	3.41	6.23	2.40	1.82	0.03	10.35
γ' phase	65.69	7.72	0.89	0.95	5.83	8.64	9.06	0.15	1.07

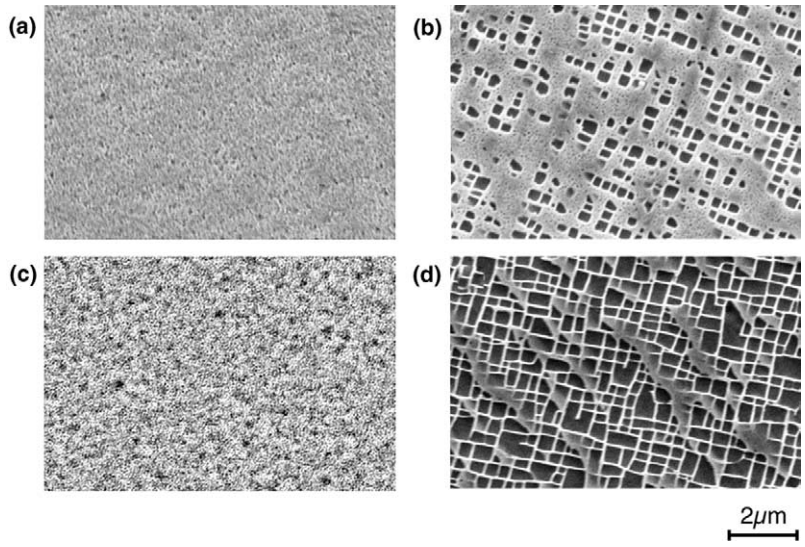

Fig. 2. Post-heat treatment microstructure of: (a) γ single-phase alloy; (b) 20% γ′ alloy; (c) 40% γ′ alloy and (d) 60% γ′ alloy.

Fig. 3 represents the as-heat-treated microstructure in a superalloy designed to contain 80% γ′ phase. Three types of microstructures were observed with different shades (as indicated by b–d in Fig. 3(a)). The microstructure in region b is similar to the 60% γ′ alloy, but width of the γ channels is narrower. In region c, the γ/γ′ structure is coarser, so γ′ appears like the matrix. The wavy γ/γ′ interfaces suggest that the interfaces are in a semi-coherent state. In the interdendritic region, a single phase of γ′ was observed as a dark shades (Fig. 3(d)). It is known that the single γ′ phase region extend to the left side under a eutectic temperature in an equilibrium phase diagram of Ni-base superalloys, as shown schematically in Fig. 1. Therefore, in this alloy, it is probable that the eutectic γ/γ′ was formed in the interdendritic region during solidification and transformed to the single γ′ phase during cooling and heat treatments. This single phase of γ′ is called eutectic γ′. The existence of a large amount of eutectic γ′ indicates that this alloy cannot be solution-treated completely under the conditions applied in this study.

The as-heat-treated microstructure in the 100% γ′ alloy is shown in Fig. 4. The dendrites consisted of a γ′ phase only. There was no γ phase, however, two other types of precipitates were observed. The interdendritic regions were densely populated with round precipitates in the γ′ matrix. Plate-like precipitates were, mostly, observed in the dendrites. Generally, precipitates, called topologically close packed (TCP) phases, are formed in long annealed Ni-base superalloys, particularly in the cases of Re added alloys. The phases σ, P, μ and R are reported as TCP phases with different crystallographic structures [6,7]. In this study, round-shaped and plate-like precipitates are expected to be TCP phases, but this

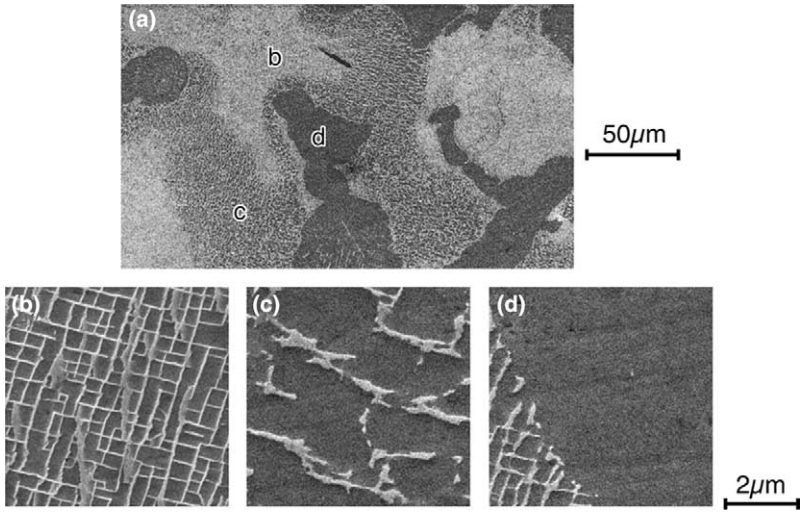

Fig. 3. Microstructure of 80% γ′ specimen after heat treatment: (a) dendritic structure; (b) fine cuboidal γ′ phases and narrow γ channels; (c) dispersed γ phases in γ′ phase and (d) γ′ single-phase area.

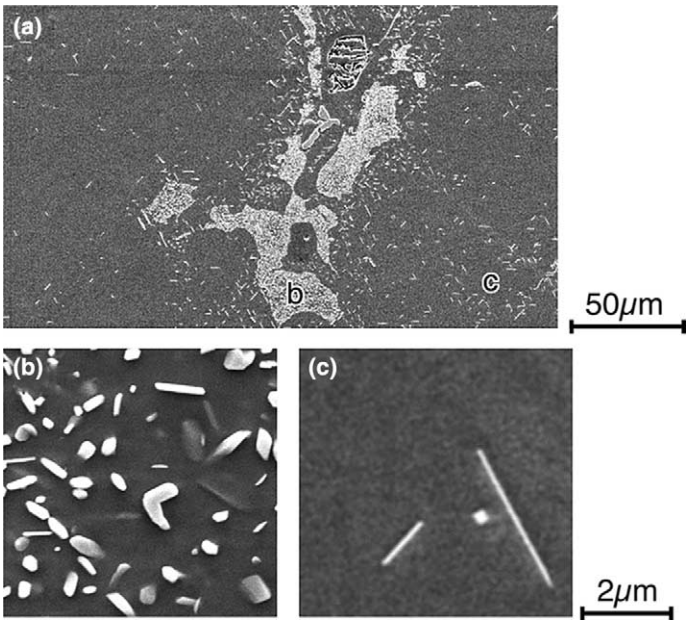

Fig. 4. Microstructure of 100% γ′ specimen after heat treatment: (a) interdendritic region; (b) round TCP phases and (c) plate-like TCP phases.

is difficult to identify clearly by EDX because the four types of TCP phases have similar compositions.

3.2. Creep rupture life

Fig. 5 shows the resultant variation of creep rupture life against the designed amount of γ′ at 900 °C, 392 MPa and 1100 °C, 137 MPa, including rupture life in standard TMS-75 (65% γ′). The results in the earlier study on Inconel 713C [1,2] are also shown for comparison. In both conditions, the single γ phase (0% γ′) TMS-75 alloys were ruptured instantly when the load was applied. The alloy containing 20% γ′ also ruptured rapidly at 1100 °C. As expected, the longest rupture life was obtained at the vicinity of 65% γ′ fraction under each condition. These results were similar to those of an earlier study, however this dependence was more evident in single crystals than in polycrystals.

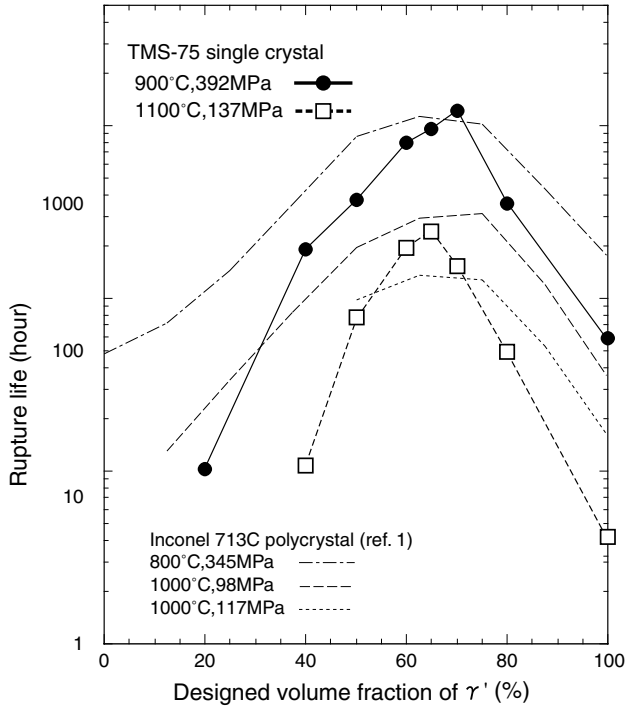

Fig. 5. Relationship between designed amount of γ′ and creep rupture life.

3.3. Microstructure after creep rupture

Fig. 6 shows the microstructure in the creep-ruptured specimens. The shape of the γ′ precipitates in the 20% γ′ alloy remained spherical after creep at 900 °C, 392 MPa for 10 h but seemed to have somewhat coarsened (Fig. 6(a)). Broad and narrow rafts perpendicular to the stress axis were observed in the 40% γ′ alloy which crept at 900 °C (Fig. 6(b)). This result means that not only cuboidal but also fine γ′ precipitates can form rafts during creep. As shown in Fig. 6(c), only broad wavy rafts were observed after creep at 1100 °C and the fine γ′ precipitates should have re-dissolved into the γ matrix under this condition. In the 60% γ′ alloys (Fig. 6(d) and (e)), the microstructure is almost the same to that reported in detail before [8]. Rafting takes place gradually at 900 °C, 392 MPa in the third generation single-crystal superalloys, however, rafting is very fast at 1100 °C, 137 MPa. Flat rafts remain in the steady creep region and are sheared at tertiary creep region.

In the 80% γ′ alloys, the direction of the rafts is quite different from that in the 40–60% γ′ alloys. At 900 °C,

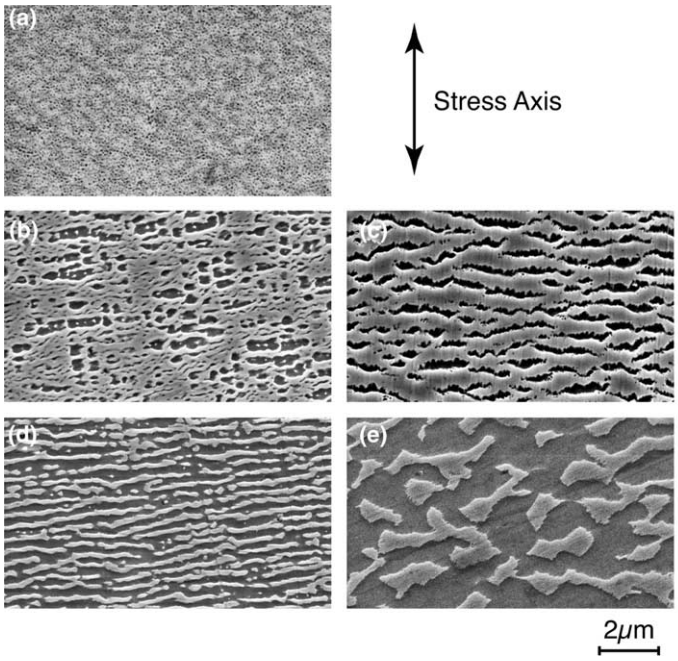

Fig. 6. Microstructure after creep rupture: the stress axis is vertical direction: (a) 20% γ' alloy at 900 °C; (b) 40% γ' alloy at 900 °C; (c) 40% γ' alloy at 1100 °C; (d) 60% γ' alloy at 900 °C and (e) 60% γ' alloy at 1100 °C.

392 MPa, fine flat rafts formed in the dendrites parallel to the stress axis, as shown in Fig. 7(a). Interdendritic regions consisted of only the γ' phase, as in the as-heat-treated microstructure. At 1100 °C, 137 MPa, parallel rafts were also observed in the dendrites, however, the microstructure was coarser and the interfaces of the rafts were wavy in the ruptured specimen (Fig. 7(b)). Rafts parallel to the stress axis have already been reported in compressed Ni-base single-crystal superalloys having a negative lattice misfit [9–11] and in the tensile creep of Ni-base alloys with a positive lattice misfit [12,13]. In this study, creep tests were performed under tension, with the lattice misfit of TMS-75 being −0.15% at 900 °C and −0.18 at 1100 °C, as previously reported [8]. This is the first time that a raft structure parallel to the loading axis has been observed under such conditions. The formation mechanism of these parallel rafts is discussed in later. In the 100% γ' alloys, the raft structure was not formed because of the absence of γ phase. At 900 °C (Fig. 7(c)), some of the plate-like TCP phases were cut to pieces, but the shapes of the rounded TCP phases in the interdendritic region were unchanged from the as-heat-treated microstructure. At 1100 °C, the shearing of plate-like TCP phases was observed more

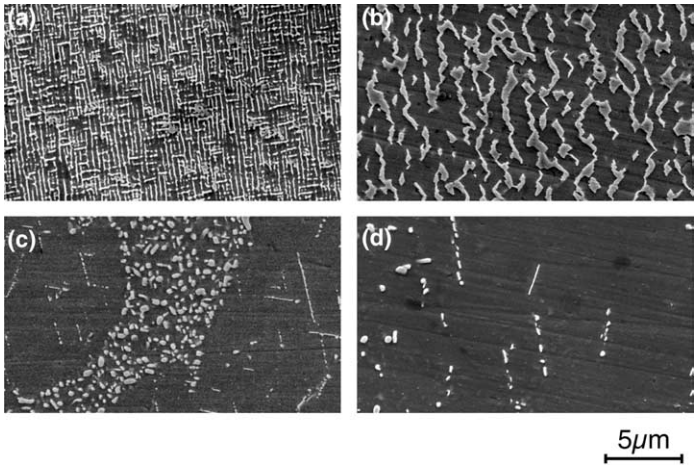

Fig. 7. Microstructure after creep rupture: the stress axis is vertical direction: (a) 80% γ' alloy at 900 °C; (b) 80% γ' alloy at 1100 °C; (c) 100% γ' alloy at 900 °C and (d) 100% γ' alloy at 1100 °C.

frequently, as shown in Fig. 6(d). In both conditions, cracks were observed at interdendritic regions near the rupture surface.

4. Discussion

4.1. Creep strength of tie line alloys

An instant rupture of some alloys means that the ultimate tensile strength was the same or smaller than the creep stress at both 900 and 1100 °C conditions, namely due to the very low viscous resistance for dislocation motion in the γ phase was very low in spite of the large quantities of solution hardening elements that were added. The single γ' phase alloy did not rupture instantly, but its creep rupture life was short. While the single-phase alloys were soft, the longest life was obtained at the 65–70% γ' fraction under both conditions. In the light of these facts, it can be said that Ni-base superalloys are strengthened by the γ/γ' interface rather than dispersed hard precipitates.

In tie line alloys, the chemical composition in each phase are kept fairly the same, but the fractions of the γ and γ' phases are different. If the same number of cuboidal γ' precipitates were dispersed and the volume fraction of γ' was changed, the Ni-base alloy would be expected to be stronger, with an increase in the γ' fraction, because the γ channels would become narrower. However, the creep test of the tie line alloys revealed that the creep rupture life decreases with an increasing amount of γ' when the fraction is over 80%. From the observation of the as-heat-treated microstructure, it was found that the heat treatment cannot fully dissolve the elements in the alloys containing over 80% γ'. In such a cases, the eutectic γ' appears in the interdendritic regions. Increasing the γ' fraction over 80% decreases the gross area of the γ/γ' interfaces, and consequently, the creep strength also decreases.

The coherency between the matrix and the precipitates has a significant influence on the creep behaviour. Generally, the creep strength of Ni-base superalloys decreases when the γ/γ' interfaces in the as-heat-treated microstructure are semi-coherent. The coarse two-phase region observed in the 80% γ' alloy is considered to be in a semi-coherent state because the interfaces are rounded and wavy. This can be attributed to the increase in the creep rate because the semi-coherent interfaces act as dislocation sources.

To consider the role of volume fraction in the creep behaviour, it is required to confirm actual volume fraction because volume fraction should change according to temperature. After heat treatment at 900 and 1100 °C for 4 h and a subsequent water quench, the volume fraction in each alloy was investigated by a point-count method, as shown in Fig. 8. The measured

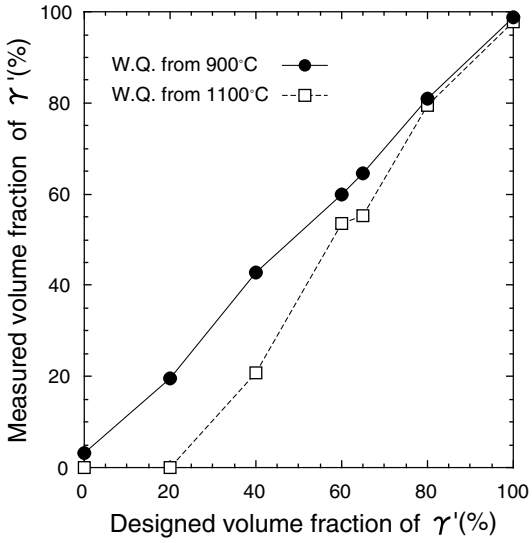

Fig. 8. Relationship between designed amount of γ' and measured amount of γ'.

volume fraction in the specimens quenched from 900 °C shows good accordance with the designed amount of γ'. In cases of alloys quenched from 1100 °C, the volume fraction of γ' decreased. The 0% and 20% alloys contain almost no γ' phase at 1100 °C. However, the decrease in γ' was small in 60–80% alloys and the microstructure in 100% alloys did not show a difference. These experimental facts mean that the γ single-phase area in the pseudo-binary phase diagram expands as the temperature increases, but the boundary line between the γ' single-phase area and the $\gamma + \gamma'$ two-phase area does not change significantly, as shown in Fig. 1.

Fig. 9 represents the relationship of the creep rupture life and measured volume fraction of γ'. The

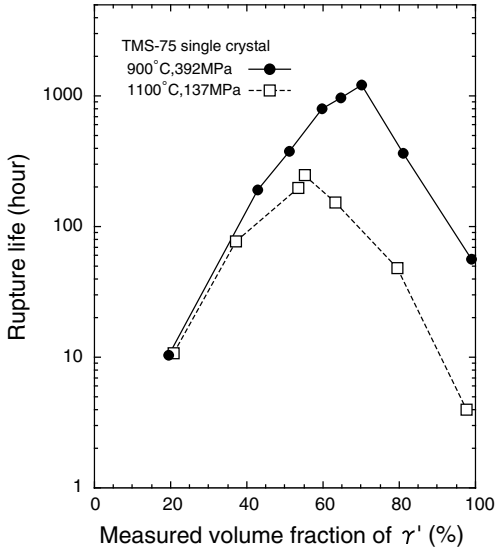

Fig. 9. Relationship between measured amount of γ' and creep rupture life.

longest rupture life was obtained with the 70% and 55% measured γ' volume fraction at 900 and 1100 °C, respectively. At 1100 °C, the maximum creep strength was achieved at 55% of the measured γ' volume fraction. This experimental fact suggests that the creep mechanisms at 900 and 1100 °C are different. At 900 °C, initial microstructure after heat-treatment is maintained for a long time and rafting take place in the later stage of creep. Therefore, it is effective for strengthening at 900 °C to prevent the dislocation motion by producing narrower γ channel without eutectic γ' region.

On the other hand, above 1100 °C, it is difficult to maintain the heat-treated microstructure during creep and rafting occurs in the very early stage of creep. When the creep stress is high enough, the shearing of rafts takes place easily and creep rupture life should be very short. However, if the creep stress is not high enough, the formed raft structure is stable. Consequently, the steady creep region and creep rupture life should extend. A stable structure is considered to contain a long flat raft with a dense interfacial dislocation network, as concluded in previous studies [14,15]. In addition to this characteristic, in this study, it was found that a raft structure has a high stability if it consists of nearly equal amount of γ and γ' phases. It is reasonable to consider that the stability of the raft structure is affected by the volume faction of γ'. If the practical volume fraction of either phase is excessive, rafts of the other phase should become thinner. It is expected that the thinner rafts are sheared to pieces more easily. Once the shear of rafts occurs, the raft structure must collapse with increasing creep rate because of decrease in gross area of the interface.

4.2. Formation of parallel rafts

Rafting arises from applied stress, lattice misfit and elastic misfit [13]. In a typical modern Ni-base single-crystal superalloy with a negative lattice misfit, rafts are formed perpendicularly to the tensile stress. On the other hand, several researcher have observed rafts parallel to the stress axis in compression creep [9–11] and in tensile creep of Ni-base alloys with a positive lattice misfit [12,13]. In this study, a raft structure was not observed in the 20% γ' alloy which crept at 900 °C. It is possible that the rupture life was too short for rafting in this case. Ordinary perpendicular rafts were observed in the 40–60% γ' alloys, whereas parallel rafts were observed in the 80% γ' alloy.

This interesting change of rafting direction can be explained, as drawn in Fig. 10. As is well known, an alloy has a negative lattice misfit and consists of a γ matrix and γ' precipitates, perpendicular rafts are formed. However, in an alloy containing dispersed γ phases in the γ' phase, parallel rafts can be formed because the lattice misfit is expected to be changed to positive from negative by the interchanges in the relative role between the matrix and the dispersed phase. In practice, the as-heat-treated microstructure of an 80% γ' alloy is not homogeneous; however, this situation can be suited for the coarsened γ/γ' two-phase structure observed in dendrite as shown in Fig. 3(c). This coarsened area is expected to expand during creep.

When plastic flow can be neglected, a driving force for rafting is affected also by the elastic misfit, m. A reversal in the sign of $m\delta\sigma$ change the type of rafting (δ, lattice misfit and σ, applied stress) [16]. According to this criterion, the driving force acts to produce perpendicular rafts in the tensile creep of an alloy containing

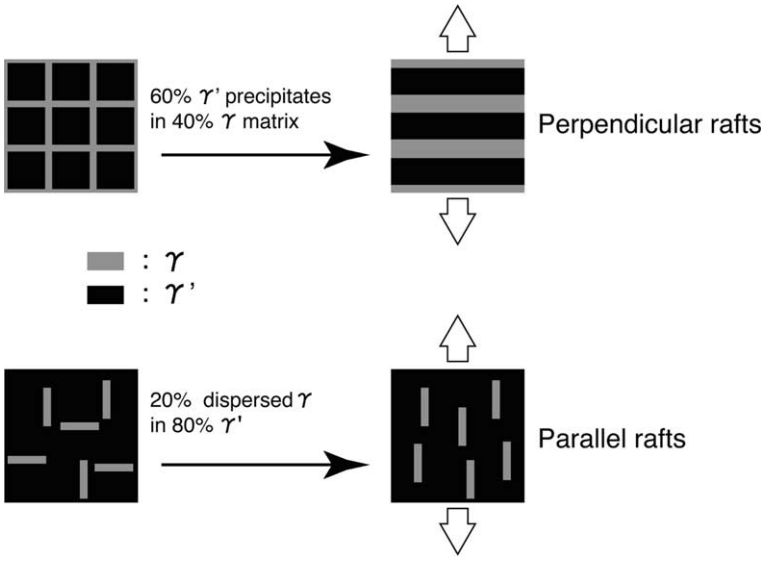

Fig. 10. Schematic drawing of formation of perpendicular and parallel rafts.

dispersed γ phases in a γ' matrix. Calculated maps for stable shapes of coherent precipitates [17,18] also predicted that a perpendicular raft is stable under such a condition. However, it should be noted that these arguments are limited to an elastic regime. On the other hand, the direction of the raft is controlled by the sign of $\sigma\delta$ in a plastic regime [16], so a parallel raft becomes stable, as actually observed in an 80% γ' alloy. If the 80% γ' alloy were crept by a lower stress at a higher temperature, a perpendicular raft may be observed in a very early stage of creep.

5. Conclusions

Creep tests at 900 °C, 392 MPa and 1100 °C, 137 MPa were performed on a third generation Ni-base single-crystal superalloy TMS-75 and its γ/γ' tie line alloys, and the microstructure of these alloys was observed by SEM. The summary is as follows:

- The γ' volume fraction of the as-heat-treated microstructure was in accordance with the original design values. The 0–60% γ' alloys have an almost homogeneous microstructure; however, there were inhomogeneities in the dendrite and interdendritic regions in the 80–100% γ' alloys.
- The longest rupture life was attained by an alloy with γ' content in vicinity of 65–70% in both creep condition. However, in comparison with measured amount of γ', the creep rupture lives were the longest at about 70% and 55% measured γ' volume fraction at 900 and 1100 °C, respectively. In addition, the dependence of the creep rupture life on the amount of γ' was more evident in single crystal than in polycrystal.
- In a ruptured specimen, a raft structure perpendicular to the stress axis was observed in the 40–60% γ' alloys. On the other hand, parallel rafts were observed in the 80% γ' alloy. The change of raft direction with increasing γ' fraction was observed for the first time in this study.
- This parallel raft structure can be explained by the interchanges in the relative role between the matrix and the dispersed phase.

References

[1] Harada H, Yamazaki M, Koizumi Y, Sakuma N, Furuya N, Kamiya H. High temperature alloys for gas turbines 1982. Forschungszentrum Jülich; 1982. p. 721.
[2] Ro Y, Koizumi Y, Harada H. Mater Sci Eng A 1997;223:59.
[3] Kobayashi T, Koizumi Y, Nakazawa S, Yamagata T, Harada H. In: Proceedings of the 4th International Charles Parsons Turbine Conference on Advances in Turbine Materials, Design and Manufacturing; 1996. p. 766.
[4] Harada H, Yokokawa T, Ohno K, Yamagata T, Yamazaki M. High temperature materials for power engineering 1990. Forschungszentrum Jülich; 1990. p. 1387.
[5] Harada H, Yamagata T, Yokokawa T, Ohno K, Yamazaki M. In: Proceedings of the 5th International Conference on Creep and Fracture of Engineering Materials and Structures; 1993. p. 255.
[6] Darolia R, Lahrman DF, Field RD. Superalloys 1988. Warrandele, PA: TMS; 1988. p. 255.
[7] Rae CMF, Karunaratne MSA, Small CJ, Broomfield RW, Jones CN, Reed RC. Superalloys 2000. Warrandele, PA: TMS; 2000. p. 767.
[8] Murakumo T, Kobayashi T, Nakazawa S, Koizumi Y, Harada H. Proc of 2nd International Symposium 'High Temperature Materials 2001'. Tsukuba, Japan: NIMS; 2001. p. 18.
[9] Véron M, Bréchet Y, Louchet F. Superalloys 1996. Warrandele, PA: TMS; 1996. p. 181.
[10] Tien JK, Copley SM. Metall Trans 1971;2:215.
[11] Tien JK, Gamble RP. Metall Trans 1972;3:2157.
[12] Pollock TM, Argon AS. Acta Metall Mater 1994;42:1859.
[13] Miyazaki T, Nakamura K, Mori H. J Mater Sci 1979;14:1827.
[14] Zhang JX, Murakumo T, Harada H, Koizumi Y. Scripta Mater 2003;48:287.
[15] Zhang JX, Murakumo T, Koizumi Y, Harada H. J Mater Sci 2003;38:4883.
[16] Nabarro FRN. Metall Mater Trans A 1996;27A:513.
[17] Pineau A. Acta Metall 1976;24:559.
[18] Onaka S, Fujii T, Suzuki Y, Kato M. Mater Sci Eng A 2000;285:246.